

# SCIENTIFIC REPORTS



OPEN

## Amyloid $\beta$ -dependent mitochondrial toxicity in mouse microglia requires P2X7 receptor expression and is prevented by nimodipine

Paola Chiozzi<sup>1</sup>, Alba Clara Sarti<sup>1</sup>, Juana M. Sanz<sup>2</sup>, Anna Lisa Giuliani<sup>1</sup>, Elena Adinolfi<sup>1</sup>, Valentina Vultaggio-Poma<sup>1</sup>, Simonetta Falzoni<sup>1</sup> & Francesco Di Virgilio<sup>1</sup> 

Previous data from our laboratory show that expression of the P2X7 receptor (P2X7R) is needed for amyloid  $\beta$  (A $\beta$ )-stimulated microglia activation and IL-1 $\beta$  release *in vitro* and *in vivo*. We also showed that A $\beta$ -dependent stimulation is inhibited by the dihydropyridine nimodipine at an intracellular site distal to the P2X7R. In the present study, we used the N13 microglia cell line and mouse primary microglia from wt and *P2rx7*-deleted mice to test the effect of nimodipine on amyloid  $\beta$  (A $\beta$ )-dependent NLRP3 inflammasome expression and function, and on mitochondrial energy metabolism. Our data show that in microglia A $\beta$  causes P2X7R-dependent a) NF $\kappa$ B activation; b) NLRP3 inflammasome expression and function; c) mitochondria toxicity; and these changes are fully inhibited by nimodipine. Our study shows that nimodipine is a powerful blocker of cell damage caused by monomeric and oligomeric A $\beta$ , points to the mitochondria as a crucial target, and underlines the permissive role of the P2X7R.

Alzheimer's disease (AD), despite a slight decrease in incidence in developed countries over the last twenty years, is still a leading cause of dementia world-wide<sup>1</sup>. About 95% of AD cases are sporadic and occur in patients over 60 years of age (late-onset AD), while about 5% are familial, and occur at a much earlier age (even at 30 years)<sup>1</sup>. Familial AD shows autosomal dominance in at least one of three main genes: amyloid precursor protein, Presenilin 1 or Presenilin 2<sup>2</sup>. The histopathological hallmark is deposition of aggregates of amyloid  $\beta$  (A $\beta$ ) peptides in the extracellular space, and intracellular accumulation of neurofibrillary tangles<sup>2</sup>. These extracellular and intracellular changes are thought to cause progressive synaptic deficit and neuronal death. The pathogenic mechanism responsible for A $\beta$ -dependent neurodegeneration is largely obscure albeit it is increasingly recognized that A $\beta$ -driven inflammation has a leading role<sup>3</sup>. Several studies in the past have stressed the pathogenic relevance of A $\beta$ -stimulated TNF $\alpha$ , IL-1 $\beta$  or reactive oxygen species (ROS) accumulation in AD brains and the ensuing neuroinflammation<sup>4-6</sup>. Without doubt, the main player in neuroinflammation is microglia, with a dual role, as a protective factor responsible for clearance of extracellular A $\beta$ -fibrils, or as an injurious agent responsible for release of neurotoxic factors, in line with the known Dr. Jekyll/Mr. Hyde role of inflammation itself<sup>7,8</sup>. Acutely, A $\beta$  triggers release of inflammatory mediators from microglia, but on the long run such sustained stimulation causes an irreversible damage<sup>8,9</sup>.

The likely inflammatory pathogenesis of AD calls for the search for novel anti-inflammatory agents active across the blood-brain-barrier (BBB), but re-evaluation of older, maybe less trendy, but no doubt widely tested drugs is also warranted. Dihydropyridines are among these re-discovered drugs. Dihydropyridines are L-type calcium blockers permeable across the BBB, and widely used to treat hypertension. It has been suggested that nimodipine and nifedipine might be beneficial to increase brain blood flow, and therefore alleviate cognitive impairment in AD<sup>10</sup>, but these observations had little or no clinical follow-up. *In vitro* experiments showed a

<sup>1</sup>Department of Morphology, Surgery and Experimental Medicine, University of Ferrara, Ferrara, Italy. <sup>2</sup>Department of Medical Sciences, University of Ferrara, Ferrara, Italy. Correspondence and requests for materials should be addressed to F.D.V. (email: [fdv@unife.it](mailto:fdv@unife.it))

protective effect in neuron/microglia co-cultures, an effect putatively assigned to inhibition of  $\text{TNF}\alpha$  and IL-1 $\beta$  release<sup>11</sup>. The protective effect of dihydropyridines might be due to inhibition of L-type voltage-dependent  $\text{Ca}^{2+}$  channels<sup>12,13</sup> or to blockade of an unrelated intracellular pathway (see also ref.<sup>14</sup>). In our previous study, we observed that the massive plasma membrane depolarization caused by opening of the P2X7R in N13 microglia was not paralleled by a nimodipine-sensitive  $\text{Ca}^{2+}$  uptake, thus suggesting that L-type  $\text{Ca}^{2+}$  channels did not play a major role in P2X7R-dependent activation of this cell type<sup>9</sup>. Thus we postulated that the inhibitory activity of nimodipine was mainly due to off-target effects. Our previous *in vitro* data showed that nimodipine (and nifedipine) are powerful inhibitors of intracellular pro-IL-1 $\beta$  accumulation as well as pro-IL-1 $\beta$  cleavage and mature IL-1 $\beta$  release induced by A $\beta$  or by extracellular ATP in microglia. Very interestingly, *in vivo* nimodipine administration, at concentrations known to be routinely reached in the CNS during therapeutical administration, significantly reduced IL-1 $\beta$  accumulation triggered by intra-hippocampal A $\beta$  inoculation<sup>9</sup>. Based on these data we hypothesized that nimodipine targeted one or more intracellular pathways involved in the activation of microglia. We also previously showed that the P2X7 receptor (P2X7R) has a key role in A $\beta$ -dependent microglial activation and injury<sup>9,15</sup>. The P2X7R is a widely distributed ATP-gated plasma membrane ion channel that is receiving increasing attention as pro-inflammatory molecule associated to cytokine release and T lymphocyte differentiation<sup>16</sup>. More recently, the possible P2X7R role in AD has been highlighted<sup>17</sup>. Although it was initially thought that pathogenic activity was mainly associated to fibrillar A $\beta$ , it is now clear that soluble A $\beta$  is also toxic<sup>18,19</sup>, therefore the effect of the monomeric or oligomeric A $\beta$  is worth of investigation.

In the present study, we investigate the effect of soluble A $\beta$  on mouse microglia and show that nimodipine not only inhibits A $\beta$ -dependent NF $\kappa$ B and NLRP3 inflammasome stimulation, but also prevents A $\beta$ -mediated mitochondrial damage. In addition, we show that in microglia expression of the P2X7R is an absolute requirement for A $\beta$  pro-inflammatory activity and mitochondrial toxicity. In conclusion, our study stresses the role of the P2X7R in A $\beta$ -dependent microglial cell damage, shows that mitochondria are a crucial target and highlights the potential benefit of nimodipine as therapeutic agent.

## Results

Amyloid  $\beta$ , but not the scrambled A $\beta$  peptide (iA $\beta$ ) is a powerful stimulus for intracellular accumulation of IL-1 $\beta$  in mouse microglia<sup>15</sup>. This effect is largely dependent on the expression of the P2X7R since it was strongly reduced in mouse microglia isolated from *P2rx7*-deleted mice (Fig. 1a). As previously shown by our laboratory<sup>9</sup>, pre-incubation with nimodipine inhibited A $\beta$ -dependent release of mature IL-1 $\beta$  as well as intracellular IL-1 $\beta$  accumulation (Fig. 1b and Supplementary Fig. S1). The main stimulus for pro-IL-1 $\beta$  accumulation is activation of the transcription factor NF $\kappa$ B. Effect of nimodipine on NF $\kappa$ B activation was tested in N13 mouse microglia, a cell line that can be easily grown to make available a sufficient amount of intracellular substrates for NF $\kappa$ B measurements. N13 cells are available as the wt and the P2X7R-low variant, selected and fully characterized in our laboratory for reduced P2X7R expression<sup>20</sup>. This variant is referred to as N13R, where R stands for "ATP-resistant". Figure 1c shows that in wt N13 microglia A $\beta$ , but not iA $\beta$ , caused a strong activation of NF $\kappa$ B that was significantly reduced by nimodipine. Intriguingly, we observed that levels of activated NF $\kappa$ B were about 3 folds higher in N13R than in wt N13 microglia, and were significantly reduced by nimodipine (Fig. 1d). Nimodipine also antagonized the small increase caused by A $\beta$  in N13R cells. Addition of iA $\beta$  had no effect. These same data are shown in Fig. 1e,f as percent increase over resting levels in wt N13 and N13R cells, respectively. Besides nimodipine, other dihydropyridines such as nifedipine and nitrendipine also inhibited A $\beta$ -stimulated IL-1 $\beta$  release (Supplementary Fig. S2). To verify whether dihydropyridine effect might be due to inhibition of voltage-gated  $\text{Ca}^{2+}$  channels reported to be expressed in mouse microglia<sup>12,13</sup>, we checked the effect on intracellular  $\text{Ca}^{2+}$  of plasma membrane depolarization. As shown in Supplementary Fig. S3, addition of KCl to N13 microglia caused no increases in the intracellular  $\text{Ca}^{2+}$  concentration, suggesting that this cell line expressed no functional voltage-gated  $\text{Ca}^{2+}$  channels. Besides causing accumulation of intracellular IL-1 $\beta$ , A $\beta$  is also a potent stimulus for pro-IL-1 $\beta$  cleavage and secretion of the mature form, both effects being effectively inhibited by nimodipine<sup>9</sup>. Pro-IL-1 $\beta$  cleavage and mature IL-1 $\beta$  secretion are independent of NF $\kappa$ B activation, and due to stimulation of the NLRP3 inflammasome<sup>21</sup>. Thus, we checked the effect of A $\beta$  and nimodipine on NLRP3 inflammasome. Figure 2a–c show that A $\beta$ , but not iA $\beta$ , caused an increase in NLRP3 protein expression in wt N13 but not in N13R cells. Enhanced expression of NLRP3 was inhibited by nimodipine, alone or in combination with an anti-oxidant such as vitamin E (Vit E). Levels of the coupling factor apoptosis-associated speck-like protein containing a CARD (ASC) were low in both wt N13 and N13R under resting conditions, were not further increased by A $\beta$  stimulation, and nimodipine had no effect under all conditions tested (not shown). Alongside with NLRP3 expression, A $\beta$  also triggered caspase-1 (casp-1) activation in wt N13 cells, whether stimulated according to the standard protocol involving LPS priming (Fig. 2d), or in the absence of LPS priming (Fig. 2e). Of note, LPS alone had no effect on casp-1 activation (Fig. 2d). A $\beta$  caused a stimulation of casp-1 similar to that triggered by ATP, a strong agonist for casp-1 activation. Nimodipine largely inhibited casp-1 activation, in both A $\beta$ - and ATP-stimulated cells, to a level comparable to that of the canonical casp-1 blocker YVAD (Fig. 2d). N13R cells were much less sensitive to casp-1 stimulation by A $\beta$  or by ATP in all conditions tested, but also in these cells nimodipine significantly decreased casp-1 activation. As shown in Fig. 2e, A $\beta$  was also a potent stimulus for casp-1 activation in the absence of LPS-priming, and its effects were largely inhibited by nimodipine. Association of nimodipine with an anti-oxidant such as Vit E did not further inhibit casp-1 activity. Nimodipine also inhibited A $\beta$ -stimulated casp-1 activation in primary microglia (Fig. 2f).

At variance with the massive inhibitory effect on IL-1 $\beta$  secretion, nimodipine had no effect on  $\text{TNF}\alpha$  secretion stimulated by LPS and A $\beta$  (Supplementary Fig S4).

The main pathway leading to NLRP3 inflammasome activation is the fast decrease in the cytosolic  $\text{K}^{+}$  concentration caused by opening of large conductance plasma membrane channels such as pannexin-1, connexins or the P2X7R itself<sup>16,22</sup>. However, it is unlikely that nimodipine hampers NLRP3 inflammasome activation by

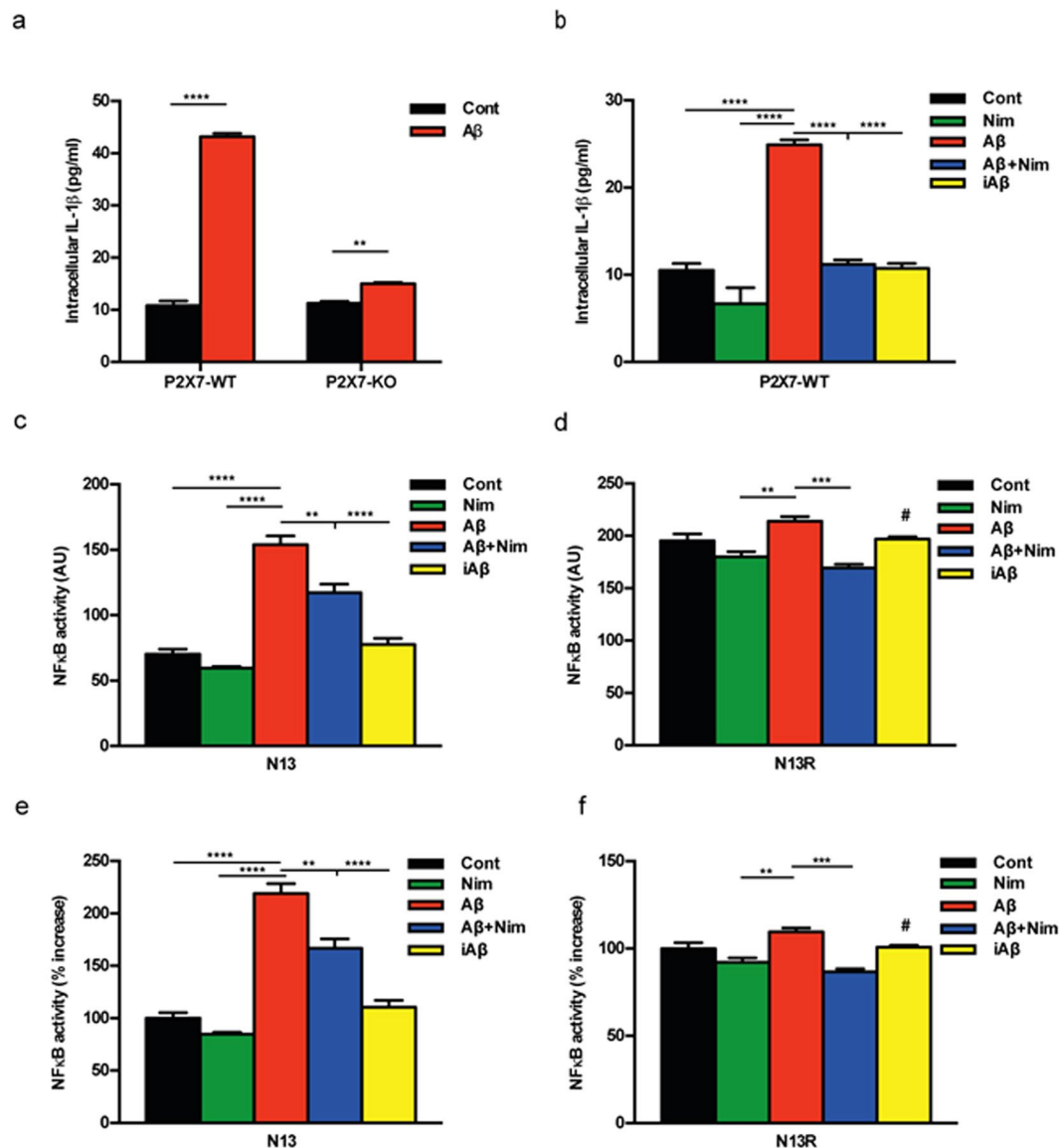


**Figure 1.** The P2X7R is an absolute requirement for Aβ-dependent microglia activation. Primary mouse microglia (a,b), suspended in 200 μl of FCS-supplemented astrocyte-conditioned medium was plated in 48-well culture dishes at a concentration of  $2 \times 10^4$ /well, and stimulated for 24 h at 37°C with the various agents as indicated. At the end, cells were rinsed, suspended in FCS-free RPMI, lysed and analysed for IL-1β content (a,b). For NFκB measurement, wt N13 or N13R cells were seeded in 10-cm Petri dishes, at a concentration of  $10^6$ /dish, treated for 24 h at 37°C with the various stimuli, and processed as described in Methods (c-f). Stimulant concentration was: Aβ, 4 μM; iAβ, 4 μM; nimodipine (nim), 36 nM. Data are means ± SEM from 3 to 5 independent experiments, each performed in triplicate, for a total of 9 to 15 individual determinations. \*\*p < 0.01; \*\*\*p < 0.001; \*\*\*\*p < 0.0001; # not significant versus controls.

interfering with plasma membrane ion fluxes, as we previously showed that plasma membrane potential changes and  $\text{Ca}^{2+}$  fluxes in microglia were not affected by nimodipine<sup>9</sup>. Another known stimulus for NLRP3 inflammasome activation is mitochondrial generation of reactive oxygen species (ROS)<sup>23</sup>. Therefore, we investigated whether nimodipine might prevent NLRP3 inflammasome activation by interfering with Aβ-dependent changes of mitochondrial energy metabolism and ROS generation. Aβ is known to cause mitochondrial toxicity witnessed by plasma membrane potential collapse, fragmentation of the mitochondrial network and overall decrease of ATP synthetic activity<sup>24</sup>. In the experiments shown in Fig. 3a,b, N13 microglial cells were incubated in the presence of Aβ for 24 h, then rinsed and loaded with the mitochondrial potential sensitive dye tetramethylrhodamine methylester (TMRM) to stain the mitochondrial network. Our anticipation was that Aβ should cause a mitochondrial potential collapse, but to our surprise, Aβ caused instead a large mitochondrial potential increase that was fully inhibited by the un-coupler FCCP, thus validating the specific mitochondrial localization of the dye. The scrambled iAβ peptide was fully inactive. The Aβ-stimulated potential increase was prevented by pre-treatment with nimodipine. Basal mitochondrial potential in quiescent cells was also slightly reduced by nimodipine.

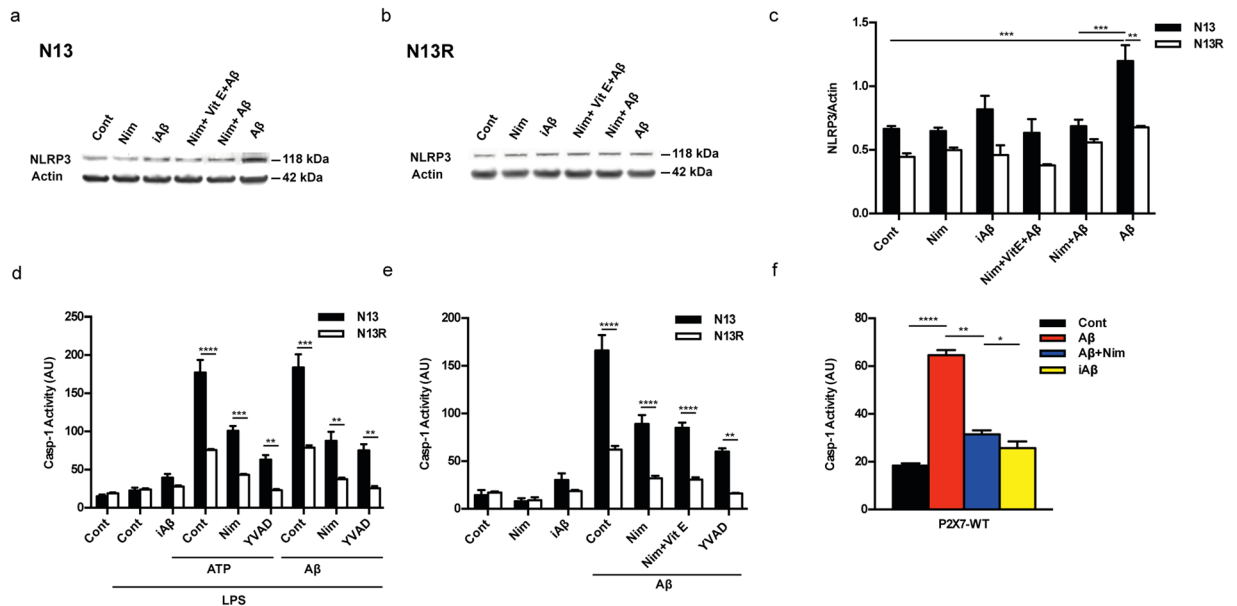


**Figure 2.** The P2X7R is needed for A $\beta$ -mediated activation of the NLRP3 inflammasome: inhibition by nimodipine. (a–e) wt N13 and N13R cells were suspended in 300  $\mu$ l of FCS-supplemented RPMI medium, plated in 24 well culture dishes at a concentration of  $1.5 \times 10^4$ /well. (f) Primary microglia was suspended in astrocyte-conditioned medium and processed as for N13 cells. In (a,b,e,f) cells were incubated for 24 h in the continuous presence of the various stimulants, while in **d** incubation was carried for a total of 5.5 h. Densitometric analysis of NLRP3 protein expression (c). ATP- and A $\beta$ -stimulated casp-1 activation in the presence (d) and absence (e) of LPS pre-treatment. Effect of nimodipine on casp-1 activation in primary microglia (f). YVAD was 50  $\mu$ M, Vit E 50  $\mu$ M, ATP 3 mM; concentration of other stimulants was as in Fig. 1, except in panel d, where A $\beta$  and iA $\beta$  were 10  $\mu$ M. Cells were pretreated with LPS in complete RPMI (wt N13 and N13R cells), after 4 h cells were rinsed and suspended in FCS-free RPMI; where indicated, nimodipine or YVAD were added, and after 1 h of incubation, cells were challenged with iA $\beta$ , A $\beta$  or ATP, then stimulated with either ATP or A $\beta$  for 30 min. YVAD, Vit E, nimodipine (nim) or nimodipine plus Vit E were added 1 h before the addition of ATP or A $\beta$ , whether in the presence or absence of LPS treatment. Data are means  $\pm$  SEM from 3 separate experiments each performed in triplicate, for a total of 9 individual determinations. \* $p < 0.05$ ; \*\* $p < 0.01$ ; \*\*\* $p < 0.001$ ; \*\*\*\* $p < 0.0001$ .

Nimodipine effect was potentiated by the anti-oxidant Vit E. We previously reported that lack of the P2X7R protects mouse microglial cells from the injurious effect of A $\beta$ <sup>15</sup>. Figure 4a,b shows that N13R cells had a lower mitochondrial potential, as previously reported in cells lacking the P2X7R<sup>25</sup>, which was only slightly increased by A $\beta$  stimulation. Nimodipine caused a significant drop of mitochondrial potential that was further collapsed by FCCP. A $\beta$  treatment also caused a large increase in mitochondrial potential in primary wt microglia, which was largely inhibited by nimodipine (Fig. 5a,b). Microglia isolated from P2X7R-deleted mice, similarly to N13R cells, showed a very thin mitochondrial network and small (but statistically significant) mitochondrial response to A $\beta$  stimulation (Fig. 6a,b). A $\beta$  is known to promote mitochondrial ROS production<sup>26</sup>. Supplementary Fig. S5 shows that A $\beta$  triggered a small but statistically significant increase in ROS production in N13 microglia. Expression of the P2X7R was also required since N13R cells showed no increase in ROS generation following A $\beta$  stimulation. As a control, we tested ATP that caused a very large, P2X7R-dependent, ROS generation.

The increase of mitochondrial potential due to short-term A $\beta$  stimulation, albeit unanticipated, suggested that ATP synthesis might be enhanced under these conditions as in principle hyperpolarization is suggestive of a tighter mitochondrial coupling and therefore more efficient oxidative phosphorylation. We initially analysed mitochondrial respiratory parameters in microglial cells with the Seahorse apparatus but we were consistently unable to obtain reproducible results in the presence of the amyloid peptide. Therefore, we simply measured total intracellular ATP content in microglia cultures after stimulation with A $\beta$  (Supplementary Fig. S6). Incubation in the presence of A $\beta$  for 5 and 24 h caused a significant decrease in total cellular ATP content, which was paralleled by a modest increase in LDH release, a gross index of cell injury. Incubation in the presence of nimodipine partially rescued the ATP drop and completely prevented LDH release.

The finding that A $\beta$  treatment hyperpolarized the mitochondria and at the same time decreased cellular ATP content is intriguing as it is anticipated that mitochondria with a higher membrane potential should synthesize more ATP. However, it is also known that the mitochondrial poison oligomycin, a selective blocker of the mitochondrial F0/F1 ATP synthase<sup>27</sup> causes at the same time hyperpolarization of mitochondrial potential and inhibition of ATP synthesis. Thus we hypothesized that A $\beta$  might have an oligomycin-like activity. To test this hypothesis we measured F0F1 activity in isolated mitochondria. We isolated a sufficient amount of mitochondria from wt N13 or N13R cells, but we found it very difficult to obtain a sufficient amount of primary microglia for mitochondria isolation, especially from P2X7R-KO pups. Therefore, to allow recovery of an amount of F0F1 complex sufficient to carry out

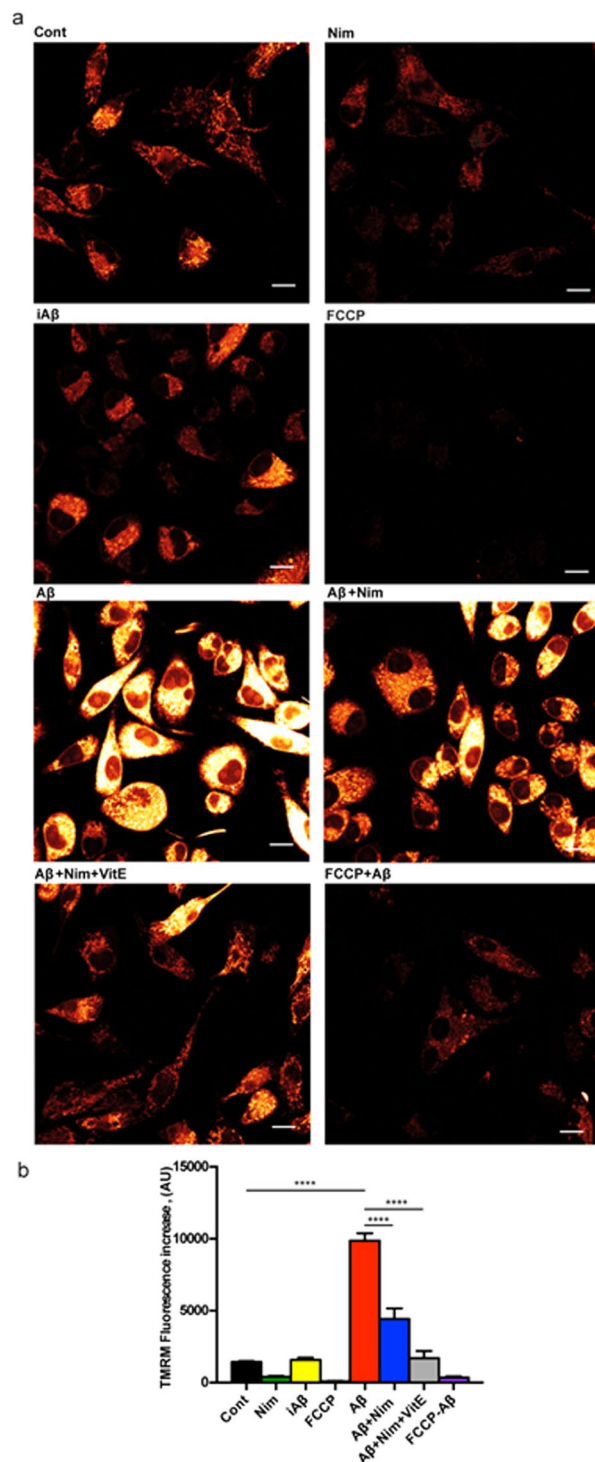


**Figure 3.** A $\beta$  drives mitochondrial hyperpolarization in wt N13 microglia: inhibition by nimodipine. Microglia cells were suspended in 1 mL of FCS-supplemented RPMI medium at a concentration of  $10^5$ /mL, and seeded onto glass coverslip slides at 37 °C for 24 h; at the end of this incubation, cells were rinsed, suspended in FCS-free RPMI and the positively charged, potential sensitive dye TMRM was added. Dishes were analyzed at confocal microscopy and single cell fluorescence was acquired (see Methods). FCCP concentration was 1  $\mu$ M; other stimulants concentration as in Figs 1 and 2. (a) Confocal microscopy pictures; bar = 10  $\mu$ m. (b) Mean fluorescence emission  $\pm$  SEM from 5 separate experiments each performed in triplicate for a total of 15 individual determinations. \*\*\*\* $p < 0.0001$ .

biochemical analysis, we isolated mitochondria from livers of P2X7R wt and P2X7R-KO mice besides wt N13 and N13R cells (Fig. 7). Mitochondria were permeabilized to freely access the F0F1 catalytic site and uncouple the ATP synthase from the respiratory chain. Incubation of isolated mitochondria in the presence of A $\beta$  strongly inhibited



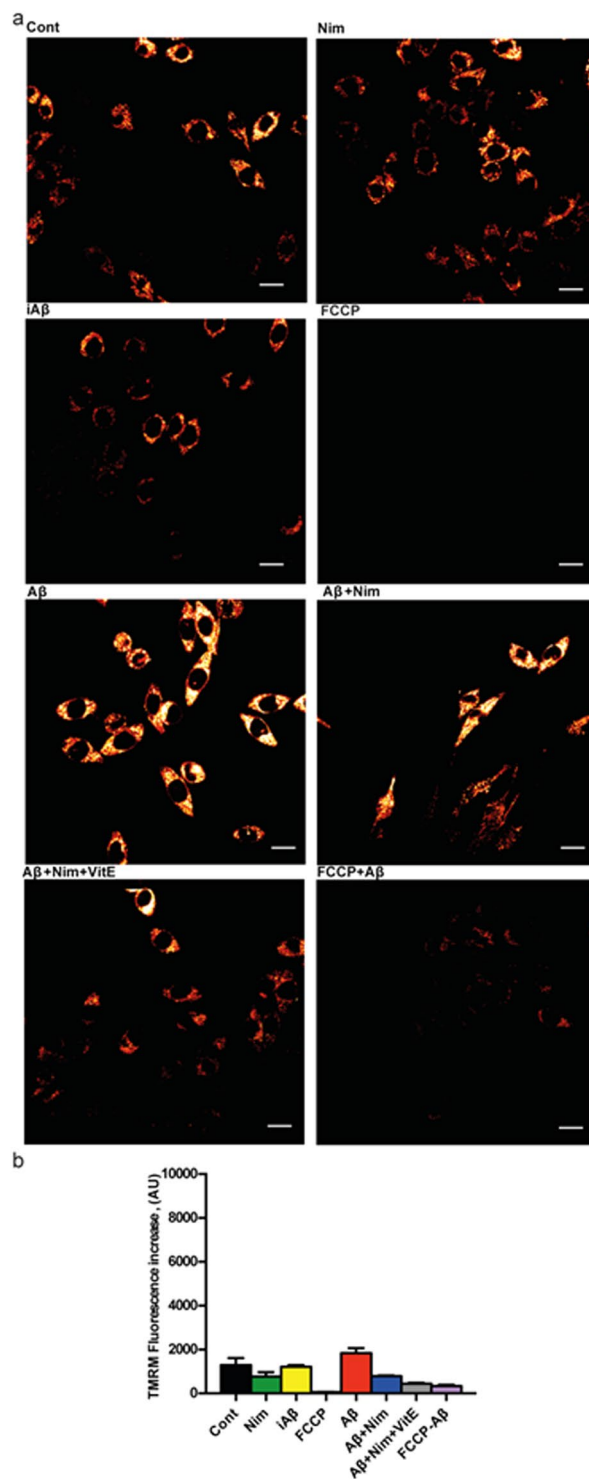


**Figure 4.** A $\beta$  does not trigger mitochondrial hyperpolarization in N13R microglia. Microglia cells were suspended in 1 mL of FCS-supplemented RPMI medium and processed as described in Fig. 3. Agonist concentration and other experimental details as in Fig. 3. **(a)** Confocal microscopy pictures; bar = 15  $\mu$ m. **(b)** Mean fluorescence emission  $\pm$  SEM from 3 independent experiments, each performed in triplicate for a total of 9 individual determinations.

ATP synthase activity in both wt N13 and N13R microglia. Interestingly, mitochondria isolated from N13R cells or P2X7R-KO liver were as sensitive to the inhibitory effect of A $\beta$  as those isolated from wt N13 cells or P2X7R wt liver. The scrambled iA $\beta$  peptide had no effect. Nimodipine was unable to prevent A $\beta$ -dependent changes in isolated mitochondria. These and our previous data<sup>9</sup> suggest that interference with mitochondrial energy metabolism might be one of the mechanisms by which A $\beta$  impairs microglia responses.

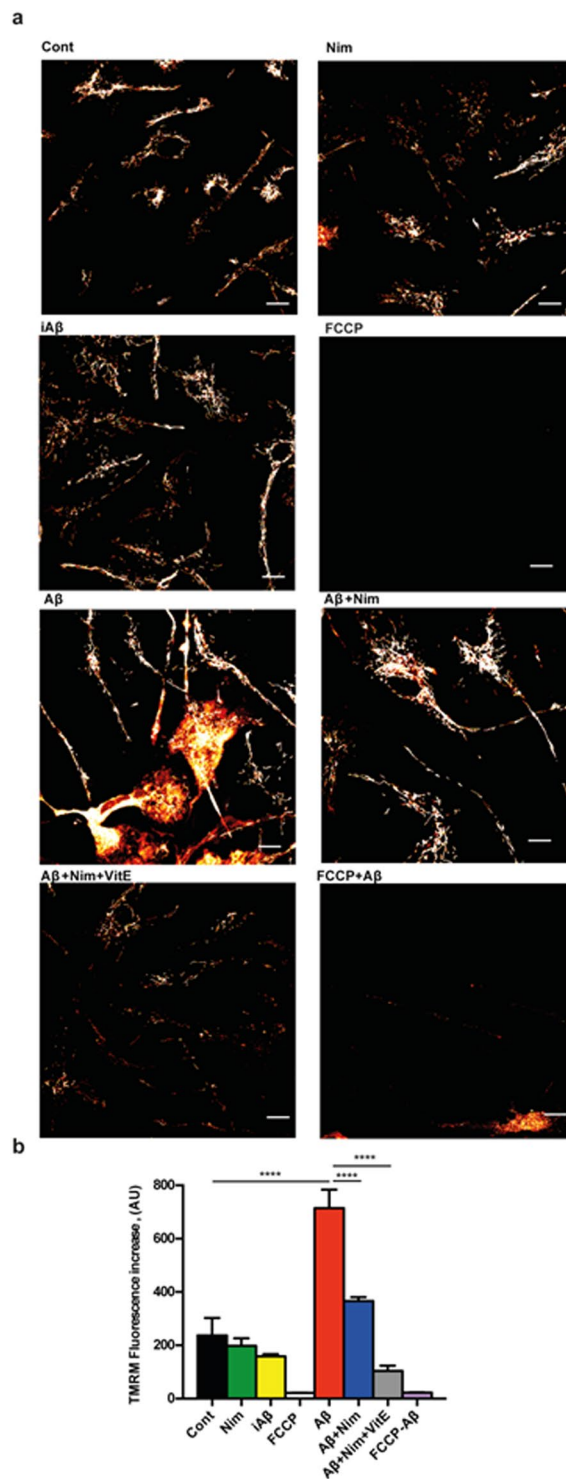


**Figure 5.** A $\beta$  drives mitochondrial hyperpolarization in primary wt microglia: inhibition by nimodipine. Microglia cells were suspended in 1 mL of astrocyte-conditioned medium, plated at a concentration of  $5 \times 10^4$ /mL, seeded onto glass coverslip slides at 37°C for 24 h and processed as described in Fig. 3. Stimulant concentration as in Fig. 3. Bar = 10  $\mu$ m. **(a)** Confocal microscopy pictures. **(b)** Mean fluorescence emission  $\pm$  SEM from 3 independent experiments, each performed in triplicate for a total of 9 individual determinations. \*\*\*\* $p < 0.0001$ .

It is known that A $\beta$ -mediated mitochondrial toxicity is heralded by cytochrome c (cyt c) release<sup>28</sup>, a key event in apoptosis, therefore we asked whether this response was triggered by A $\beta$  in microglia, and possibly inhibited by nimodipine. As shown in Fig. 8a,b, nimodipine by itself slightly but significantly prevented basal cyt c release from the mitochondria and in parallel reduced its accumulation into the cytosol of resting wt N13 microglia. A $\beta$

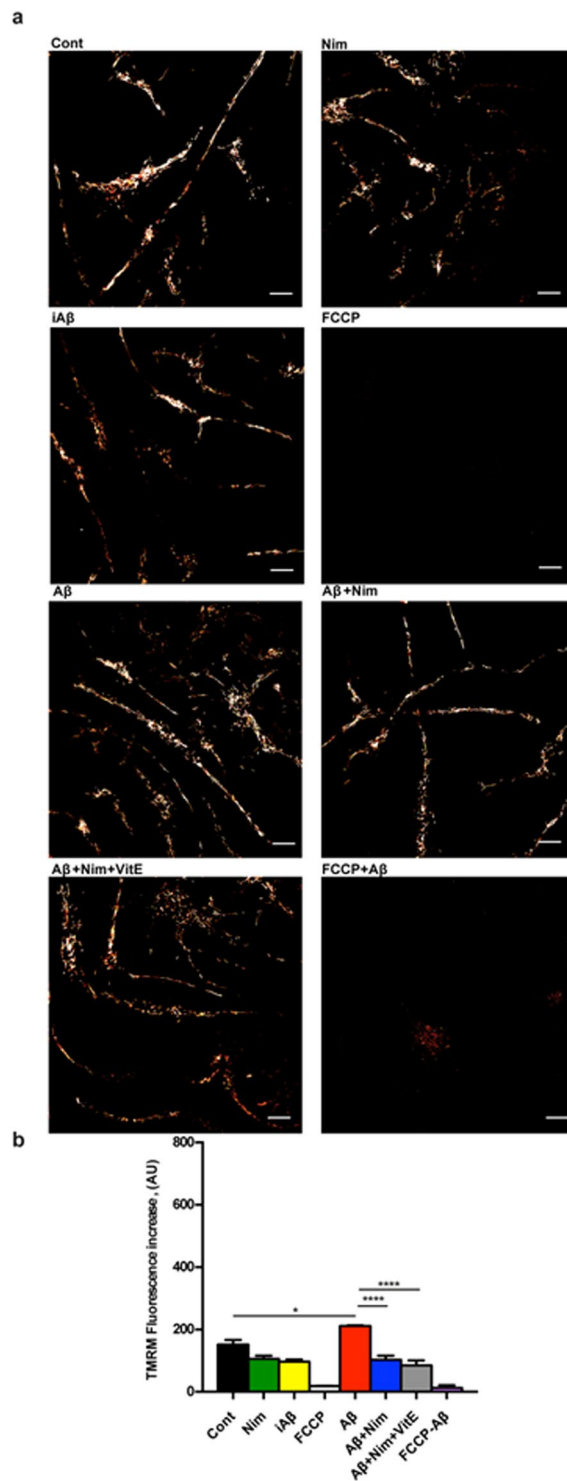
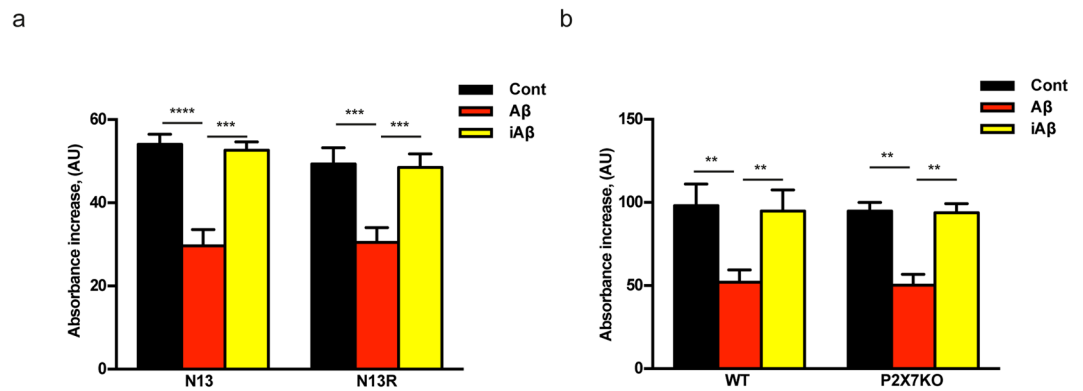


**Figure 6.** A $\beta$  drives a reduced mitochondrial hyperpolarization in P2X7R-deleted primary microglia. Microglia cells were suspended in 1 mL of astrocyte-conditioned medium, plated at a concentration of  $5 \times 10^4$ /mL on glass coverslip slides at 37 °C for 24 h, and processed as in Fig. 3. Stimulant concentration as in Fig. 3. **(a)** Confocal microscopy pictures; bar = 10  $\mu$ m. **(b)** Mean fluorescence emission  $\pm$  SEM from 3 independent experiments, each performed in triplicate for a total of 9 individual determinations. \* $p < 0.05$ ; \*\*\*\* $p < 0.0001$ .

caused a strong stimulation of cyt c release from the mitochondria and a large accumulation in the cytosol, which were both prevented by nimodipine. The scrambled iA $\beta$  peptide had no effect. In the N13R cells, A $\beta$ -triggered an about 30% lower cyt c release compared to wt N13 microglia (Fig. 8c). In both wt N13 and N13R cells in parallel with release from mitochondria, cyt c accumulated into the cytoplasm (Fig. 8d), to a slightly lower level in wt N13 microglia. This was surprising since we anticipated that cytoplasmic cyt c should be higher in wt N13 versus





N13R cells since the amount of cyt c released from the mitochondria in wt N13 was about 30% higher than in N13R cells (Fig. 8c). Thus, we asked if some of the cyt c released was removed from the cytoplasm in wt N13 but not in N13R microglia.

Since activated microglia is known to release plasma membrane-derived microvesicles<sup>29</sup>, we hypothesized that cytoplasmic cyt c might be trapped and released via these particles. Figure 8e shows that stimulation of wt N13 or N13R cells with A $\beta$  triggered release of microvesicles that could be collected in the cell supernatants according to current procedures<sup>29,30</sup>. Although P2X7R stimulation is known to trigger a large release of plasma membrane-derived microvesicles from microglia as well other cell types<sup>29,30</sup>, A $\beta$ -driven microvesicle shedding was marginally affected by lack of P2X7R (Fig. 8f). Shed microvesicles are known to contain a plethora of cytoplasmic or membrane-associated molecules, such as NLRP3 inflammasome components, MHC-I and-II molecules, metalloproteases, as well as ATP receptors (e.g. P2X7R itself)<sup>29,30</sup>. Data from Fig. 8e show that microvesicles also contained cyt c. Although a precise estimate of the amount of cyt c contained in the microvesicles is not possible, our data strongly suggest that the lower content of cytoplasmic cyt c in wt N13 versus N13R cells depended on cyt c being trapped within shed microvesicles in wt N13 but not N13R microglia, thus resulting in an amount of microvesicle-associated cyt c many fold lower in N13R versus wt N13 microglia (Fig. 8g,h). Note that values on the y axis in Fig. 8h are ten times lower than in Fig. 8g. Microvesicles released from N13R cells also had a very low P2X7R content (Fig. 8e). Overall microvesicles release was similar in N13R and wt N13 cells. Thus, data in Fig. 8 show that stimulation of microglia cells with A $\beta$  triggered a large release of cyt c from the mitochondria, which was in part sequestered within shed microvesicles. Sequestration of cyt c within the microvesicles only occurred in the presence of the P2X7R. Nimodipine had no effect on microvesicle release whether in the absence or presence of A $\beta$ , but drastically reduced basal and A $\beta$ -stimulated microvesicle cyt c content (Fig. 8e).

It is known that P2X7R may promote phagocytosis in microglia<sup>31</sup> and ATP stimulation promotes pinocytosis<sup>32</sup>, thus we investigated whether the protective effect afforded by P2X7R deletion might depend on a reduced pinocytic uptake of A $\beta$ , and whether this might also explain the protective effect of nimodipine. As shown in Supplementary Fig S7 N13R cells did show a reduced pinocytic uptake of Texas red-labelled ovalbumin, but this is unlikely to explain the protective effect of nimodipine as in the presence of this drug pinocytosis was basically unaffected.

## Discussion

Despite the enormous expenditure of efforts and financial resources in the investigation of Alzheimer's disease, payback in terms of novel efficacious drugs has been highly disappointing<sup>1</sup>. This might be one of the reasons behind the recent decision of a major Pharmaceutical Company such as Pfizer to withdraw from Alzheimer's research<sup>33</sup>. Such years-long and deluding search suggests that identification of novel cellular targets, intracellular pathways and candidate pharmacological compounds is absolutely needed. Identification of the molecular mechanism of A $\beta$ -dependent toxicity is a hot focus in Alzheimer's research. This misfolded protein is understood to have both a direct neuronal cell-centred effect and a broader microglia-targeted pro-inflammatory activity<sup>34</sup>. Accruing observations show that mitochondrial dysfunction is often found in Alzheimer's patients, thus raising the issue of an A $\beta$ -mediated impairment of mitochondrial oxidative phosphorylation<sup>35–37</sup>. Previous studies focused on alterations in mitochondrial respiratory complexes, mainly complex IV (cytochrome c oxidase), the mitochondrial permeability transition pore (mPTP)<sup>38</sup>, and more recently on the F0F1 ATP synthase<sup>37</sup>. In this latter study, mitochondria localized at neuronal synapses were found to be exquisitely sensitive to A $\beta$ -mediated damage due to selective removal of the oligomycin sensitivity-conferring protein (OSCP) of the ATP synthase complex<sup>37</sup>. A $\beta$  accumulates in mitochondria of neuronal cells very likely via the translocase of outer membrane (TOM) and putatively localizes to mitochondrial cristae<sup>39</sup>. It is not known whether mitochondrial toxicity might also underlie A $\beta$ -mediated injury of non-neuronal cells.

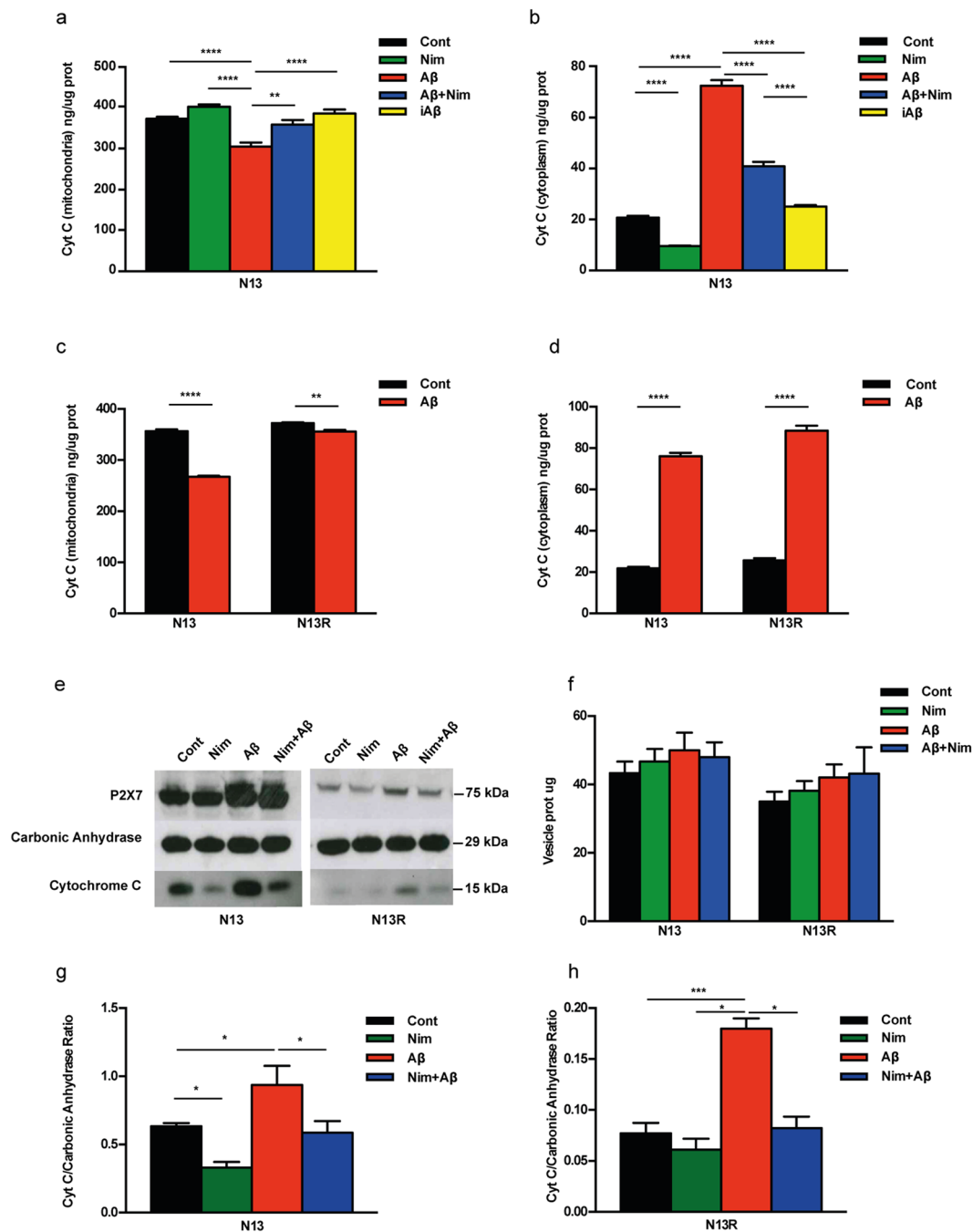


**Figure 8.** A $\beta$  triggers cyt c release from mitochondria in N13 cells. (a–d) Microglia was suspended in complete RPMI medium, plated in 10 cm Petri dishes at a concentration of  $10^6$ /dish for 24 h at 37°C, and challenged with the various stimuli. Cytochrome c (cyt c) was analyzed as described in Methods. (e–h) Microglia cells were maintained in FCS-supplemented RPMI at for 24 h 37°C at a concentration of  $5 \times 10^5$ /dish, then the various stimulants were added at the concentration reported in Fig. 1. At the end, supernatants were withdrawn and microvesicles collected as detailed in Methods. Microvesicle suspensions were concentrated to 0.5–1 mg/mL, loaded onto SDS-PAGE and probed for P2X7R and cyt c content. Carbonic anhydrase (1  $\mu$ g) was exogenously added to the microvesicle suspensions and used as loading standard. Strips were cut from the same blot and probed with the relevant antibodies against the P2X7R, carbonic anhydrase or cytochrome c. (f) Microvesicle release from N13 and N13R cells ( $\mu$ g/ $5 \times 10^5$  cells). (g,h) Densitometric analysis of microvesicle cyt c content normalized on the carbonic anhydrase. Data from (a–d) are means  $\pm$  SEM from 3 to 4 independent experiments, each performed in six replicates for a total of 18 to 24 individual determinations. Data from (f–h) are means  $\pm$  SEM from 4 independent experiments. Blot shown in (e) is exemplificative of 4 similar. \* $p < 0.05$ ; \*\* $p < 0.01$ ; \*\*\* $p < 0.001$ ; \*\*\*\* $p < 0.0001$ .

Microglia is now generally acknowledged to be an additional important target of A $\beta$ -dependent toxicity, but the pathogenic mechanisms are far from clear. In fact, microglia has a dual effect on AD pathogenesis, a detrimental activity dependent on release of neurotoxic factors such as ROS, cytokines, chemokines or metalloproteases, and a protective function based on microglia ability to remove A $\beta$  or accelerate its degradation<sup>34,40</sup>. However, it is increasingly evident that in AD microglia is unable to fulfil its phagocytic tasks, but the mechanism underlying this dysfunction is unknown<sup>41</sup>. In the present study, we show that in mouse microglia A $\beta$  severely hampered mitochondrial energy metabolism by targeting the F0F1 ATP synthase, thus resulting in 50% reduction of activity and in about 30% decrease of total ATP content over a 24 h incubation. Interestingly, A $\beta$  treatment did not significantly affect the function of the respiratory chain, but rather caused hyperpolarization of the mitochondria, as it would be anticipated on the basis of an oligomycin-like effect. Despite the undisputed contribution to phagocytosis of anaerobic glycolysis, it is clear since the very early studies by Cohn<sup>32</sup> that oxidative metabolism is also required, thus mitochondrial dysfunction could seriously impair removal of extracellular particulate matter. Therefore, we think that mitochondrial dysfunction triggered by A $\beta$  causes a complex dysregulation of microglia functions characterized on one hand by an acute stimulation of pro-inflammatory cytokine release, and on the other on a long term reduction of phagocytic activity, and therefore of removal of extracellular A $\beta$  fibrils. However, A $\beta$  needs the cooperation of an additional partner to successfully injure microglia: the P2X7R.

We previously showed that in mouse microglia A $\beta$ -dependent release of the pro-inflammatory cytokine IL-1 $\beta$  is strictly dependent on expression of a functional P2X7R, likely due to direct interaction of the amyloid peptide with this receptor<sup>15</sup>. Here we further extend these early observations by showing that A $\beta$ -dependent NLRP3 gene transcription and NLRP3 inflammasome stimulation were also P2X7R-mediated. Thus, in microglia the whole A $\beta$ -stimulated, inflammasome-associated, pro-inflammatory machinery was P2X7R-dependent. Even more interestingly, our findings show that also mitochondrial dysfunction in microglia was P2X7R dependent. N13R cells or primary microglia lacking the P2X7R were resistant to A $\beta$ -dependent mitochondrial hyperpolarization. In addition, N13R cells were also resistant to A $\beta$ -triggered cyt c release, another event heralding mitochondrial toxicity.

Based on our previous study suggesting a direct interaction of A $\beta$  with the P2X7R<sup>15</sup>, we hypothesize that the P2X7R facilitates A $\beta$  cellular uptake and mitochondrial localization, and therefore is permissive for mitochondrial injury. The P2X7R is reported to have scavenger activity independent of its pore-forming function, possibly relevant in the central nervous system<sup>42,43</sup>, and to promote endocytosis of extracellular anti-bacterial peptides (e.g. LL-37)<sup>44</sup>. Extracellular ATP is long known to stimulate pinocytosis<sup>32</sup>, and more recently basal activity of the P2X7R was shown to promote innate phagocytosis<sup>45</sup>. Thus, it is conceivable that the facilitating role of the P2X7R in supporting A $\beta$ -dependent toxicity resides in its promotion of pinocytosis or innate phagocytosis, as shown in Suppl Fig S7. In support of this view, lack of the P2X7R did not prevent A $\beta$  inhibition of F1/F0 ATP synthase activity in isolated and permeabilized mitochondria, showing that once the mitochondria are freely accessible to A $\beta$  lack of the P2X7R has no protective effect, nor there is an intrinsic P2X7R-associated F1/F0 ATP synthase defect.

Search for effective therapies for AD has been substantially fruitless. This failure underscores the need to identify novel targets and drugs. A few year ago we reported that the well-known voltage-gated Ca<sup>2+</sup> channel blockers nimodipine and nitrendipine fully inhibited A $\beta$ -stimulated IL-1 $\beta$  release from mouse microglia<sup>9</sup>. Since brain microglia does not express functional L-type Ca<sup>2+</sup> channels, we hypothesized off-target effects of the dihydropyridine compounds. Data shown in the present study support this hypothesis as nimodipine strongly reduced all A $\beta$ -dependent effects, i.e. NF $\kappa$ B activation, NLRP3 inflammasome stimulation, IL-1 $\beta$  release, mitochondrial dysfunction and LDH and cyt c release. Other members of the dihydropyridine family, i.e. nifedipine and nitrendipine, also inhibited A $\beta$ -stimulated IL-1 $\beta$  release, and like nimodipine had no effect on A $\beta$  stimulated TNF $\alpha$  release. We don't think that nimodipine directly antagonizes the P2X7R since early responses such as Ca<sup>2+</sup> influx and uptake of extracellular fluorescent markers are unaffected<sup>9</sup>, but we rather believe that it targets a pathway downhill to the P2X7R, although we have no evidence so far of the molecular identity of this pathway. Mitochondria are an attractive target, although the finding that nimodipine had no protective effect on isolated mitochondria speaks against a direct protective effects towards A $\beta$ -mediated inhibition of F0F1 ATP synthase. More likely, nimodipine prevented delivery of A $\beta$  to the mitochondria. However, this protective effect is not due to inhibition of pinocytic uptake as nimodipine causes, if any think, a modest increase in pinocytosis. Thus, we hypothesize that nimodipine might accelerate endosome-lysosome fusion, and therefore A $\beta$  degradation, but at the moment we have no proof for this. Here we show that, whichever the pathway by which A $\beta$  reaches the mitochondria, mitochondrial dysregulation is at basis of the wide-range activation of inflammatory responses, i.e. NF $\kappa$ B activation, NLRP3 expression, casp-1 activation and IL-1 $\beta$  maturation and release<sup>46</sup>. Thus, nimodipine by preventing A $\beta$ -dependent mitochondrial toxicity, prevents the activation of several key pro-inflammatory pathways.

In summary, this study highlights a novel pathway for the inhibition of microglia cell functions by A $\beta$ , further underlines the key role of the P2X7R as a permissive factor for A $\beta$  toxicity in mouse microglia, and demonstrates the potent protective effect of nimodipine. We showed previously that nimodipine prevents *in vivo* intra-hippocampal accumulation of IL-1 $\beta$  triggered by A $\beta$  inoculation<sup>9</sup>, thus nimodipine administration might be a viable therapeutic strategy for AD.

## Methods

**Cells.** Microglial N13 cells were grown in RPMI-1640 medium, heretofore referred to as RPMI medium, supplemented with 2 mM glutamine, 10% fetal calf serum (FCS) (Gifco BRL, Basel, Switzerland), 100 U/ mL penicillin and 100 mg/mL streptomycin. Primary mouse microglia cells were isolated from 2 to 4-day-old post-natal mice as described previously<sup>15</sup>. More than 98% of cells were identified as microglia using a macrophage cell-specific F4/80 biotinylated mAb antibody (Serotec, Dusseldorf, Germany) followed by staining with Oregon Green 488 goat anti-rat IgG (Molecular Probes, Leiden, The Netherlands). All animal care and experimental procedures complied with institutional and national guidelines (see below). Microglia were plated in astrocyte-conditioned medium (high glucose-DMEM supplemented with 2 mM glutaMAX<sup>TM</sup> (Gibco Life Technologies Europe BV,

Monza, Italy), 10% FCS, 100 U/mL penicillin and 100 mg/mL streptomycin), and used for experiments 24 h after plating. Short-term experiments were run either in FCS-free RPMI medium or in a saline solution with the following composition: 125 mM NaCl, 5 mM KCl, 1 mM MgSO<sub>4</sub>, 1 mM NaH<sub>2</sub>PO<sub>4</sub>, 20 mM HEPES, 5.5 mM glucose, 5 mM NaHCO<sub>3</sub>, 1 mM CaCl<sub>2</sub>, pH 7.4. Nimodipine, nitrendipine and nifedipine (Sigma-Aldrich Srl, Milano, Italy), were dissolved in dimethyl sulfoxide at a concentration of 10 mg/mL. Long-term (chronic) experiments were performed in FCS-supplemented RPMI medium (complete RPMI) (wt N13 and N13R cells), or in astrocyte-conditioned medium (primary microglia). All experiments were performed at 37 °C. Lipopolysaccharide (LPS) from *Escherichia coli* serotype 055:B5 (Sigma-Aldrich) was dissolved in PBS at a concentration of 1 mg/ml. A $\beta$  1–42 and the inactive scrambled A $\beta$  peptide (iAb) 42–1 were purchased from Bachem (Bubendorf, Switzerland). A $\beta$  peptides were dissolved in dimethyl sulfoxide at a concentration of 1 mM. Freshly prepared A $\beta$  solution used in the experiments (final concentrations from 4 to 10  $\mu$ M) mainly consists of monomers/oligomers, as witnessed by staining (Supplementary Fig S8).

**Animals.** Procedures involving animals and their care were conducted in conformity with the institutional guidelines that are in compliance with national (D.lgs. n. 26/2014), and international laws and policies (EU Directive 86/609/EEC; Guide for the Care and Use of Laboratory Animals, U.S. National Research Council, 1996), and were approved by the Italian Ministry of Health (authorizations n. 75/2013 released on 25/03/2013, 716/2016-PR released on 18/05/2016, and 744/2018-PR released on 01/09/2018).

All efforts were made to minimize the number of animals used and their suffering. The results of all studies involving animals are reported in accordance with the ARRIVE guidelines for reporting experiments involving animals. *Ex vivo* samples used in this study were from a total of 32 C57Bl/6 wt (Envigo-Harlan Laboratories, Udine, Italy) or *P2rx7*-KO female mice (kind gift of GlaxoSmithKlein, UK) weighing 18–20 g. They were housed in the animal facility of the University of Ferrara at constant room temperature (22  $\pm$  1 °C) and relative humidity (55  $\pm$  5%) under a 12 h light/dark cycle (lights on from 7:00 AM to 7:00 PM). Food and water were freely available.

**Isolation of mitochondria.** Mitochondria from wt N13 or N13R cell cultures or from mouse livers were isolated as described by Wieckowski *et al.*<sup>47</sup>. For isolation from livers, 6-week old C57Bl/6 (male) mice were sacrificed by cervical dislocation, livers extracted and minced at 4 °C in about 10 volumes of BSA-containing mannose-sucrose-hepes-EDTA (MSHE) buffer<sup>47</sup>, and rinsed several times to remove blood. All following procedures were performed at 4 °C. Tissue was homogenised by applying 10 strokes of a drill-driven Teflon glass homogenizer. Homogenate was centrifuged at 800 g for 10 min, fat/lipid contamination was removed by careful aspiration, and the remaining supernatant was centrifuged at 10000 g for 10 min. After removal of the light mitochondrial layer, pellet was suspended in BSA-containing MSHE, and centrifuged one more time at the same speed. The final pellet was suspended in a minimal volume of BSA-containing MSHE. Total protein concentration (mg/mL) was determined by the Bradford method (Bio-Rad Laboratories, Segrate, Milano, Italy). Typically, an amount of about 7.5 mg of mitochondria was obtained from a single mouse liver.

**Measurement of IL-1 $\beta$ , TNF $\alpha$  and of enzymatic activity.** Lactate dehydrogenase (LDH) activity was measured according to standard laboratory procedures. IL-1 $\beta$  was measured with a R&D kit (R&D, Minneapolis, MN, USA). TNF $\alpha$  was measured with a Quantikine ELISA kit (R&D). F0F1 ATP synthase activity was measured by a coupled enzyme assay in isolated mitochondria permeabilized with two rounds of freeze/thawing, and suspended in phenol red and serum-free RPMI. Briefly, mitochondria were incubated in RPMI at a concentration of 30  $\mu$ g/mL in a spectrophotometer cuvette in the presence of pyruvate kinase (0.8 U/mL), lactate dehydrogenase (1.12 U/mL), phosphoenol pyruvate (1.5 mM), antimycin A (1  $\mu$ M), rotenone (1  $\mu$ M), ATP (200  $\mu$ M) and NADH (100  $\mu$ M). ATP is hydrolysed by F0F1 ATP synthase to produce ADP that is used by pyruvate kinase to generate pyruvate at the expenses of phosphoenolpyruvate, thus regenerating ATP. Pyruvate is oxidized to lactate by lactate dehydrogenase (LDH) in the presence of NADH, that is in turn oxidized to NAD<sup>+</sup>. NADH oxidation is measured by spectrophotometry at 340 nm. F0F1 ATP synthase-independent NADH oxidation rate was measured in the presence of oligomycin (2  $\mu$ M), and subtracted from total oxidation rate.

**Measurement of NF $\kappa$ B activity.** NF $\kappa$ B activity was assessed by measuring nuclear translocation of the p65-NF $\kappa$ B subunit with the Nuclear Extraction Kit (Active Motif, Carlsbad, CA, USA) and the NF $\kappa$ B transcription Factor Assay Kit (Abcam, Cambridge, UK). Briefly, after treatment with various stimulants, cells were lysed and processed according to manufacturer's instructions. Supernatants were collected and transferred to 96-well plates coated with a specific double stranded DNA (dsDNA) sequence containing the p65-NF- $\kappa$ B response element. p65-NF- $\kappa$ B was detected by addition of specific primary antibody, and visualized by ELISA.

**Western blotting.** Cells were detached by scraping and lysed in lysis buffer (300  $\mu$ M sucrose, 1 mM K<sub>2</sub>HPO<sub>4</sub>, 1 mM MgSO<sub>4</sub>, 5.5 mM glucose, 20 mM HEPES (pH 7.4), 1 mM benzamidine, 1 mM phenylmethylsulfonyl fluoride, 0.2  $\mu$ g DNase, and 0.3  $\mu$ g RNase, all by Sigma-Aldrich) by repeated freeze/thawing cycles. Proteins were separated on Novex NuPage Bis-Tris 4–12% precast gel (Life Technologies, Milano, Italy) and transferred to nitrocellulose membranes (GE Healthcare-Life Sciences, Milano, Italy). After incubation with TBS-Tween-20 (0.1%) supplemented with 2.5% non-fat powdered milk plus 0.5% BSA for 1 h to saturate unspecific binding sites, membranes were incubated overnight with primary antibodies at 4 °C. The anti-NLRP3 polyclonal antibody (Imgenex, Bio-Techne Srl, Milano, Italy, cat. N. NBP2-12446) was diluted 1:500. The anti-actin polyclonal antibody (Sigma-Aldrich, cat. N. A5060) was diluted 1:1,000. The anti-P2X7R polyclonal antibody (Merck-Millipore, Milano, Italy, cat. n. AB5246) was diluted 1:1,000. The anti-cytochrome C monoclonal antibody (cat. n. Ab 13575, Abcam) was diluted 1:1,000 and the anti-carbonic anhydrase II (CA2) polyclonal antibody (Sigma-Aldrich, cat. n. SAB 2900749) was diluted 1:1000. Membranes were incubated with secondary goat anti-rabbit HRP-conjugated antibodies (Invitrogen-Thermo Fisher Scientific, Monza, Italy, cat. n. 31460) at a 1:3,000 dilution for 1 h at room



temperature. Densitometric analysis of the protein bands was performed with the freely available ImageJ software. Band density was normalized over the actin band. All the antibody were diluted in TBS–Tween-20 (0.1%) supplemented with 2.5% non-fat powdered milk plus 0.5% BSA.

**Intracellular Ca<sup>2+</sup> measurement.** Cytoplasmic Ca<sup>2+</sup> concentration was measured at the wavelength excitation 340/380 and emission 505 with the fluorescent indicator fura-2/AM (Thermo Fisher Scientific) in a thermostat-controlled (37 °C) and magnetically-stirred Cary Eclipse Fluorescence Spectrophotometer (Agilent Technologies, Milano, Italy). Cells were loaded with 4 μM fura-2/AM in the following saline solution: 125 mM NaCl, 5 mM KCl, 1 mM MgSO<sub>4</sub>, 1 mM NaH<sub>2</sub>PO<sub>4</sub>, 20 mM HEPES, 5.5 mM glucose, 1 mM CaCl<sub>2</sub>, pH 7.4, supplemented with 250 μM sulfinpyrazone. After loading, cells were rinsed and re-suspended at a concentration of 10<sup>6</sup>/ml in the above saline solution.

**Pinocytosis.** Pinocytosis was measured by Texas red-albumin uptake. Briefly, N13 or N13R cells were incubated in the presence of a concentration of 30 μg/ml of ovalbumin Texas red conjugate (Thermo Fisher Scientific) for 1 hour in the presence or absence of nimodipine, rinsed and then cell-associated fluorescence was measured in a Wallac Victor Perkin Elmer (Perkin Elmer, Beaconsfield, UK) plate reader. Cells were also analysed by microscopy to verify intracellular formation of pinocytotic vacuoles.

**Microscopy.** Microscopy was performed with a temperature-controlled Zeiss LSM 510 confocal microscope (Carl Zeiss, Aresa, Italy). Mitochondrial potential was measured by monitoring uptake of the positively-charged dye TMRM as previously described<sup>25</sup>. Reactive oxygen species were detected using the fluorogenic CellROX™ 488 reagent (Invitrogen), according to manufacturer's instructions. Briefly, N13 cells were seeded on 24-well plates and challenged with the different stimuli. After a 1 h incubation, the dye was then added to a concentration of 10 μM and fluorescence measured by fluorescence microscopy at an excitation wavelength of 488 nm.

**Measurement of extracellular ATP.** ATP was measured in cell lysates with the luciferase/luciferin method (Enliten luciferase/luciferin, Promega, Italy) in a Firezyme luminometer (Biomedica Diagnostics Inc, Windsor, Canada). Data are expressed as relative luminescence units (RLU), and converted into nanomoles of ATP thanks to a calibration curve performed by adding known ATP amounts.

**Microvesicle preparation.** Cells were plated in 6-well culture dishes in the absence or presence of the various stimulants at a concentration of 5 × 10<sup>5</sup>/well. Then, supernatants were withdrawn and centrifuged at 800 × g for 10 min to get rid of cells and cell debris. The supernatant was further centrifuged at 10,000 × g, and the pellet (microvesicles) lysed in a 300 mM sucrose solution supplemented with 0.1 Triton X-100 plus PMSF and benzamide. Centrifugations and further manipulations were performed at 4 °C.

**Statistical analysis.** All data are shown as means ± standard error of the mean (SEM). Test of significance was performed by two-way ANOVA using GraphPad InStat software (GraphPad, San Diego, Ca, USA).

## Data Availability

The datasets generated during and/or analyzed during the current study are available from the corresponding author on reasonable request.

## References

- Scheltens, P. *et al.* Alzheimer's disease. *Lancet* **388**, 505–517 (2016).
- Bertram, L., Lill, C. M. & Tanzi, R. E. The genetics of Alzheimer disease: back to the future. *Neuron* **68**, 270–281 (2010).
- McGeer, P. L., Rogers, J. & McGeer, E. G. Inflammation, anti-inflammatory agents and Alzheimer disease: the last 12 years. *J. Alzheimers. Dis.* **9**, 271–276 (2006).
- Michelucci, A., Heurtaux, T., Grandbarbe, L., Morga, E. & Heuschling, P. Characterization of the microglial phenotype under specific pro-inflammatory and anti-inflammatory conditions: Effects of oligomeric and fibrillar amyloid-beta. *J. Neuroimmunol.* **210**, 3–12 (2009).
- Eikelenboom, P. *et al.* Neuroinflammation - an early event in both the history and pathogenesis of Alzheimer's disease. *Neurodegener. Dis.* **7**, 38–41 (2010).
- Vandenabeele, P. & Fiers, W. Is amyloidogenesis during Alzheimer's disease due to an IL-1/IL-6-mediated 'acute phase response' in the brain? *Immunol. Today* **12**, 217–219 (1991).
- Wes, P. D., Sayed, F. A., Bard, F. & Gan, L. Targeting microglia for the treatment of Alzheimer's Disease. *Glia* **64**, 1710–1732 (2016).
- Gutierrez, A. & Vitorica, J. Toward a New Concept of Alzheimer's Disease Models: A Perspective from Neuroinflammation. *J. Alzheimers. Dis.* **64**, S329–S338 (2018).
- Sanz, J. M. *et al.* Nimodipine inhibits IL-1beta release stimulated by amyloid beta from microglia. *Br. J. Pharmacol.* **167**, 1702–1711 (2012).
- Lopez-Arrieta, J. M. & Birks, J. Nimodipine for primary degenerative, mixed and vascular dementia. *Cochrane. Database. Syst. Rev.* **CD000147** (2002).
- Li, Y., Hu, X., Liu, Y., Bao, Y. & An, L. Nimodipine protects dopaminergic neurons against inflammation-mediated degeneration through inhibition of microglial activation. *Neuropharmacology* **56**, 580–589 (2009).
- Silei, V. *et al.* Activation of microglial cells by PrP and beta-amyloid fragments raises intracellular calcium through L-type voltage sensitive calcium channels. *Brain Res.* **818**, 168–170 (1999).
- Espinosa-Parrilla, J. F., Martinez-Moreno, M., Gasull, X., Mahy, N. & Rodriguez, M. J. The L-type voltage-gated calcium channel modulates microglial pro-inflammatory activity. *Mol. Cell Neurosci.* **64**, 104–115 (2015).
- Schappel, A. *et al.* Nimodipine fosters remyelination in a mouse model of multiple sclerosis and induces microglia-specific apoptosis. *Proc. Natl. Acad. Sci. USA* **114**, E3295–E3304 (2017).
- Sanz, J. M. *et al.* Activation of microglia by amyloid {beta} requires P2X7 receptor expression. *J. Immunol.* **182**, 4378–4385 (2009).
- Di Virgilio, F., Dal Ben, D., Sarti, A. C., Giuliani, A. L. & Falzoni, S. The P2X7 Receptor in Infection and Inflammation. *Immunity* **47**, 15–31 (2017).
- Martin, E. *et al.* New role of P2X7 receptor in an Alzheimer's disease mouse model. *Mol. Psychiatry* **24**, 108–125 (2019).

18. Chiti, F. & Dobson, C. M. Protein misfolding, functional amyloid, and human disease. *Annu. Rev. Biochem.* **75**, 333–366 (2006).
19. Chiti, F. & Dobson, C. M. Protein Misfolding, Amyloid Formation, and Human Disease: A Summary of Progress Over the Last Decade. *Annu. Rev. Biochem.* **86**, 27–68 (2017).
20. Ferrari, D. *et al.* Mouse microglial cells express a plasma membrane pore gated by extracellular ATP. *J. Immunol.* **156**, 1531–1539 (1996).
21. Di Virgilio, F. The therapeutic potential of modifying inflammasomes and NOD-like receptors. *Pharmacol. Rev.* **65**, 872–905 (2013).
22. Munoz-Planillo, R. *et al.* K(+) efflux is the common trigger of NLRP3 inflammasome activation by bacterial toxins and particulate matter. *Immunity*. **38**, 1142–1153 (2013).
23. Schroder, K., Zhou, R. & Tschopp, J. The NLRP3 inflammasome: a sensor for metabolic danger? *Science* **327**, 296–300 (2010).
24. Tillement, L., Lecanu, L. & Papadopoulos, V. Alzheimer's disease: effects of beta-amyloid on mitochondria. *Mitochondrion*. **11**, 13–21 (2011).
25. Adinolfi, E. *et al.* Basal Activation of the P2X7 ATP Receptor Elevates Mitochondrial Calcium and Potential, Increases Cellular ATP Levels, and Promotes Serum-independent Growth. *Mol. Biol. Cell* **16**, 3260–3272 (2005).
26. Markesbery, W. R. Oxidative stress hypothesis in Alzheimer's disease. *Free Radic. Biol. Med.* **23**, 134–147 (1997).
27. Lardy, H. A. & Ferguson, S. M. Oxidative phosphorylation in mitochondria. *Annu. Rev. Biochem.* **38**, 991–1034 (1969).
28. Kim, H. S. *et al.* Amyloid beta peptide induces cytochrome C release from isolated mitochondria. *Neuroreport* **13**, 1989–1993 (2002).
29. Bianco, F. *et al.* Astrocyte-derived ATP induces vesicle shedding and IL-1beta release from microglia. *J. Immunol.* **174**, 7268–7277 (2005).
30. Pizzirani, C. *et al.* Stimulation of P2 receptors causes release of IL-1beta-loaded microvesicles from human dendritic cells. *Blood* **109**, 3856–3864 (2007).
31. Gu, B. J. & Wiley, J. S. P2X7 as a scavenger receptor for innate phagocytosis in the brain. *Br. J. Pharmacol.* **175**, 4195–4208 (2018).
32. Cohn, Z. A. & Parks, E. The regulation of pinocytosis in mouse macrophages. 3. The induction of vesicle formation by nucleosides and nucleotides. *J. Exp. Med.* **125**, 457–466 (1967).
33. Reuters, <https://www.reuters.com/article/us-pfizer-alzheimers/pfizer-ends-research-for-new-alzheimers-parkinsons-drugs-idUSKBN1EW0TN> (2018).
34. Balducci, C. & Forloni, G. Novel targets in Alzheimer's disease: A special focus on microglia. *Pharmacol. Res.* **130**, 402–413 (2018).
35. Reddy, P. H. Role of mitochondria in neurodegenerative diseases: mitochondria as a therapeutic target in Alzheimer's disease. *CNS. Spectr.* **14**, 8–13 (2009).
36. Swerdlow, R. H. *et al.* Mitochondria, Cybrids, Aging, and Alzheimer's Disease. *Prog. Mol. Biol. Transl. Sci.* **146**, 259–302 (2017).
37. Beck, S. J. *et al.* Deregulation of mitochondrial F1FO-ATP synthase via OSCP in Alzheimer's disease. *Nat. Commun.* **7**, 11483 (2016).
38. Du, H. & Yan, S. S. Mitochondrial permeability transition pore in Alzheimer's disease: cyclophilin D and amyloid beta. *Biochim. Biophys. Acta* **1802**, 198–204 (2010).
39. Hansson Petersen, C. A. *et al.* The amyloid beta-peptide is imported into mitochondria via the TOM import machinery and localized to mitochondrial cristae. *Proc. Natl. Acad. Sci. USA* **105**, 13145–13150 (2008).
40. Rajendran, L. & Paolicelli, R. C. Microglia-Mediated Synapse Loss in Alzheimer's Disease. *J. Neurosci.* **38**, 2911–2919 (2018).
41. Krabbe, G. *et al.* Functional impairment of microglia coincides with Beta-amyloid deposition in mice with Alzheimer-like pathology. *PLoS One* **8**, e60921 (2013).
42. Gu, B. J. *et al.* P2X7 receptor-mediated scavenger activity of mononuclear phagocytes toward non-opsonized particles and apoptotic cells is inhibited by serum glycoproteins but remains active in cerebrospinal fluid. *J. Biol. Chem.* **287**, 17318–17330 (2012).
43. Vessey, K. A. *et al.* Loss of Function of P2X7 Receptor Scavenger Activity in Aging Mice: A Novel Model for Investigating the Early Pathogenesis of Age-Related Macular Degeneration. *Am. J. Pathol.* **187**, 1670–1685 (2017).
44. Tang, X., Basavarajappa, D., Haeggstrom, J. Z. & Wan, M. P2X7 Receptor Regulates Internalization of Antimicrobial Peptide LL-37 by Human Macrophages That Promotes Intracellular Pathogen Clearance. *J. Immunol.* **195**, 1191–1201 (2015).
45. Gu, B. J., Saunders, B. M., Jursik, C. & Wiley, J. S. The P2X7-nonmuscle myosin membrane complex regulates phagocytosis of nonopsonized particles and bacteria by a pathway attenuated by extracellular ATP. *Blood* **115**, 1621–1631 (2010).
46. Banoth, B. & Cassel, S. L. Mitochondria in innate immune signaling. *Transl. Res.* **202**, 52–68 (2018).
47. Wieckowski, M. R., Giorgi, C., Lebedzinska, M., Duszyński, J. & Pinton, P. Isolation of mitochondria-associated membranes and mitochondria from animal tissues and cells. *Nat. Protoc.* **4**, 1582–1590 (2009).

## Acknowledgements

F.D.V. is supported by grants from the Italian Association for Cancer Research (n. IG 13025 and IG 18581), the Ministry of Education of Italy (PRIN 20178YTNC), and the Ministry of Health of Italy (n. RF-2011-02348435). E.A. is supported by grant from the Italian Association for Cancer Research (n. IG 16812). F.D.V., E.A. and A.L.G. are also supported by institutional funds from the University of Ferrara. This work was funded with support from the European H2020 office through the COST Action BM1406 “Ion channels and Immune response”.

## Author Contributions

F.D.V. projected this work, planned experiments and wrote the M.S., P.C. was responsible for most of the experiments. A.C.S. performed experiments aimed at measuring mitochondrial parameters, and thoroughly revised the M.S., J.M.S. and A.L.G. helped with cell cultures and W.B., E.A. performed microscopy and helped with data analysis. V.V.P. helped with cell fractionation and analysis of microvesicle content. S.F. was responsible for cell cultures and microglia isolation, and for MS revision.

## Additional Information

**Supplementary information** accompanies this paper at <https://doi.org/10.1038/s41598-019-42931-2>.

**Competing Interests:** F.D.V. is a member of the Scientific Advisory Board of Biosceptre Ltd, a UK-based Company involved in the development of P2X7-targeted antibodies, and has an ongoing collaboration with Ablynx, a Belgian Company involved in the development of P2X7R-targeted nanobodies. Other Authors declare no conflict of interest.

**Publisher's note:** Springer Nature remains neutral with regard to jurisdictional claims in published maps and institutional affiliations.





**Open Access** This article is licensed under a Creative Commons Attribution 4.0 International License, which permits use, sharing, adaptation, distribution and reproduction in any medium or format, as long as you give appropriate credit to the original author(s) and the source, provide a link to the Creative Commons license, and indicate if changes were made. The images or other third party material in this article are included in the article's Creative Commons license, unless indicated otherwise in a credit line to the material. If material is not included in the article's Creative Commons license and your intended use is not permitted by statutory regulation or exceeds the permitted use, you will need to obtain permission directly from the copyright holder. To view a copy of this license, visit <http://creativecommons.org/licenses/by/4.0/>.

© The Author(s) 2019